Deep learning for efficient frontier calculation in finance. *

Xavier Warin †

January 8, 2021

Abstract

We propose deep neural network algorithms to calculate efficient frontier in some Mean-Variance and Mean-CVaR portfolio optimization problems. We show that we are able to deal with such problems when both the dimension of the state and the dimension of the control are high. Adding some additional constraints, we compare different formulations and show that a new projected feedforward network is able to deal with some global constraints on the weights of the portfolio while outperforming classical penalization methods. All developed formulations are compared in between. Depending on the problem and its dimension, some formulations may be preferred.

Key words: Deep neural networks, finance, Mean-Variance, Mean-CVaR, effective frontier

1 Introduction

Portfolio selection in order to achieve a given expected return given an accepted risk has been a long time studied subject. The first problem studied was the one period Mean-Variance problem in [Mar52], [Mar59]. An analytic solution has been proposed first in [Mer72] for a positive covariance matrix and when short selling is allowed. It is only in [LN00] that the multi-period case has been solved by a reformulation of the problem as a linear quadratic (LQ) one. The solution for the continuous case when short selling is allowed in a complete Black Scholes market has been proposed in [ZL00] still based on the LQ reformulation. The case without short selling has been solved two years after in [LZL02]. Notice that, in this case, a solution is provided if borrowing is allowed so that the investment in the bond is not constrained. Then some extension with some randomization in coefficients is proposed in [Lim04], some risk on the correlations in [CW14], [IP19]. Very recently some results are obtained in [JMP20] supposing that the volatility is rough [GJR18] and follows some affine and quadratic Volterra model: the Mean-Variance problem is solved in some case as the explicit solution of some Riccati backward stochastic differential equations.

All these theoretical results are interesting but of limited use by practitioner as borrowing is generally not used and other operational constraints are added: investors first tend to limit the rebalancing of the portfolio (only achieved at some discrete dates) to limit transaction cost by imposing constraints on the variation of the investment weights in the assets composing the portfolio. Second, they generally impose some strategic views on the weights that are only allowed to stay in some certain limits. In this case, numerical methods are necessary. Using conventional PDE methods [WF10] have solved many constrained problems in the case of a single risky asset following a Black Scholes dynamic. The same methodology in the case of an asset with jumps

*This work is supported by FiME, Laboratoire de Finance des Marchés de l'Energie

†EDF R&D & FiME xavier.warin at edf.fr

has been used in [DF14]. This kind of approach can only be used at most with two or three assets and the resolution of a realistic portfolio selection problem is out of reach. In to order tackle the multi dimensional problem with constraints, [CO16] have proposed two algorithms based on the LQ formulation: the first being based on pure forward simulations is sub optimal with constraints, while the second using a backward recursion is based on regressions such that only rather low dimensional cases can be solved.
The used of the variance to evaluate the risk has been questioned by both practitioners and searchers as it both penalizes gain and loss. Numerous downsize risk measures penalizing losses or low gains have been proposed in the literature. Among them, Low Partial Moments (LPM) which have been proposed more than forty years ago in [Fis77] rely on two parameters : the gamma γ parameter named the "Benchmark" parameter is set by the investor and the second one q represents the risk attitude of the investor. This risk model embeds a lot of classical models. For example the case $q = 0$ corresponds to the safety rule of [Roy52], the case $q = 1$ correspond to the expected regret of [DR99], $q = 2$ corresponds to the semi deviation below the Benchmark parameter or the semi variance if the Benchmark parameter is set to the expected wealth.
Another classical risk measure related is the CVaR introduced in [RU+00] corresponding the expected loss below the VaR measure. As shown in [RU+00], CVaR calculation can be parametrized as the minimum over a parameter α of a function value linked to a LPM risk measure with parameter $q = 1$. Using this formulation, [Gao+17] studied the Mean-CVaR continuous case giving semi analytical solutions to the Mean-CVaR problem when the wealth is bounded. Indeed the boundedness of the wealth or the control as studied in [MY17] is necessary as the general case is not well posed for downsize risk measures as shown in [JYZ05]: using this kind of risk measure, and without constraints, the investors tend to gamble more and more if the market is in bad shape, and investments in the most risky assets tend toward infinity. Therefore, the Mean-CVaR problem has to be solved with constraints or in discrete time and numerical methods are necessary to optimize portfolio. A classical approach consists in using the auxiliary formulation proposed by [RU+00] and in using a gradient descend method on α as proposed in [MY17]. However, this procedure is very time consuming and only can be solved in low dimension.
In order to optimize portfolio with general Mean-Risk measure, Neural Networks appears to be an interesting choice. Neural networks are known to be able to approximate function in high dimension. Very recently, neural networks have been used in risk management first in [Bue+19]. Some cases with constraints on the hedging products and some downsize risk measures have been studied in [FMW19]. In both cases, results reported are promising. Some cases of Asset Liability Management have been reported very recently in [KT20].
In this article, we show that neural networks are able to calculate very realistic efficient frontier in the Mean-Variance case and the Mean-CVar case.
The main findings developed are the following ones:

- **Neural networks are able to solve some continuous Mean Variance problems accurately in low and high dimension for the control**: using different formulations, we first solve the continuous Mean-Variance problem without constraints in the Black Scholes model with a direct formulation and the LQ formulation. We introduce for each formulation two methods to approximate the efficient frontier : the first one approximates the frontier point by point while the second permits to evaluate the global frontier in a single calculation. In all the cases, the frontier is correctly approximated in dimension 4 and 20 by comparison to the analytical solution.
  Then we used the global and point by point local method and adapt the network to solve the problem when no short selling and borrowing are allowed. Although we do not have any analytical solution, all frontiers calculated are very similar indicating that they are correctly evaluated.

- **Neural networks are able to deal with some operational constraints**: in order to calculate the frontier when some global and local constraints are added to the resolution we propose different formulations based on different penalization methods. We show that the global constraints are hard to satisfy by penalization and we introduce a new projected feedforward network which is able to deal with the fact that the weights in the portfolio are such that all of them are positive, that their sum is equal to one and that each weights are between some given bounds. Numerical methods still indicate that the border is correctly calculated.

- **Neural networks are able to deal with the Mean Variance problem with a state in high dimension**: the Black Scholes case is interesting but is special as the state of the problem only involve the global wealth: then as the number of assets increases, only the dimension of the control increases. In a section we use some Heston model and show that the frontiers are still correctly calculated with or without constraints. As the state of the problem depends on the wealth and the variance of the assets, we have shown that we are able to solve a high dimension problem for both the state and the control.

- **Neural networks can solve some Mean-CVaR problem accurately**: we solve some more difficult Mean-CVaR problems and show that on some cases, solutions are sometimes trapped in local minima that can be far from the optimum. In this case, some multiple calculations can be achieved to get back the correct frontier for some global formulations while the point by point formulation always gives oscillations.

We also show that, depending on the problem, one formulation may be preferred:

- For the Mean-Variance problem, a point by point approximation of the frontier is the best choice for the Black Scholes model, while the global formulation is the best choice for the Heston model.

- Whereas for the Mean-CVaR, the global approach with a randomization of the risk coefficients is the only way to always obtain good results in the high dimension case (or what seems to be good results because no reference is available).

The article article is organized as follows: In the first section, we briefly recall what a neural network is, then in the second section, we solve the continuous Mean-Variance problem. Some constraints are added in the third section. Section fourth and fifth focus respectively on the use of the Heston model in the Mean-Variance setting and the Mean-CVaR setting with a Black Scholes model.
In the whole sequel, we note $(\Omega, \mathcal{F}, \mathbb{P}, \mathcal{F}_t)$ a filtered probability space. For each set $\mathcal{A}$ de $\mathbb{R}^d$, we note $\mathcal{L}^2_{\mathcal{F}_t}(0, T, \mathcal{A})$ the set of the $\mathcal{F}_t$ adapted square integrable processes with values in $\mathcal{A}$. For an element x of $\mathbb{R}$, $x^+ = \max(x, 0)$ applied component by component. At last we suppose that the risk free rate is 0 which is equivalent to discount all asset values with a rate r, so that we consider all risky assets with an adapted trend equal to the surplus of trend with respect to the non risky asset.

2 Neural networks as function approximators

Deep neural networks are designed to approximate unknown or large class of functions. They rely on the composition of simple functions, and appear to provide an efficient way to handle high-dimensional approximation problems, by finding the "optimal" parameters by stochastic gradient descent methods. We here use some basic type of network dubbed feedforward networks. We fix the input dimension $d_0 = d$ that will represent the dimension of the state variable x, the output dimension d_1 (here $d_1 = 1$ for approximating the real-valued solution to the PDE, or $d_1 = d$

for approximating the vector-valued gradient function), the global number $L+1 \in \mathbb{N} \setminus \{1,2\}$ of layers with m_ℓ, $\ell = 0, \ldots, L$, the number of neurons (units or nodes) on each layer: the first layer is the input layer with $m_0 = d$, the last layer is the output layer with $m_L = d_1$, and the $L-1$ layers between are called hidden layers, where we choose for simplicity the same dimension $m_\ell = m$, $\ell = 1, \ldots, L-1$. A feedforward neural network is a function from $\mathbb{R}^d$ to $\mathbb{R}^{d_1}$ defined as the composition

$$x \in \mathbb{R}^d \longmapsto A_L \circ \varrho \circ A_{L-1} \circ \ldots \circ \varrho \circ A_1(x) \in \mathbb{R}^{d_1}. \tag{1}$$

Here A_ℓ, $\ell = 1, \ldots, L$ are affine transformations: A_1 maps from $\mathbb{R}^d$ to $\mathbb{R}^m$, $A_2, \ldots, A_{L-1}$ map from $\mathbb{R}^m$ to $\mathbb{R}^m$, and A_L maps from $\mathbb{R}^m$ to $\mathbb{R}^{d_1}$, represented by

$$A_\ell(x) = \mathcal{W}_\ell x + \beta_\ell, \tag{2}$$

for a matrix $\mathcal{W}_\ell$ called weight, and a vector β_ℓ called bias term, $\varrho : \mathbb{R} \to \mathbb{R}$ is a nonlinear function, called activation function, and applied component-wise on the outputs of A_ℓ, i.e., $\varrho(x_1, \ldots, x_m) = (\varrho(x_1), \ldots, \varrho(x_m))$. Standard examples of activation functions are the sigmoid, the ReLU, the ELU, tanh. Generally the number of layers is kept low (between 2 and 4) in order to avoid the problem of vanishing gradient and the number of neurons depends on d but is kept generally between 10 and 100.

All these matrices $\mathcal{W}_\ell$ and vectors β_ℓ, $\ell = 1, \ldots, L$, are the parameters of the neural network, and can be identified with an element $\theta \in \mathbb{R}^{\kappa_{L,m}}$, where $\kappa_{L,m} = \sum_{\ell=0}^{L-1} m_\ell(1 + m_{\ell+1}) = d(1 + m) + m(1 + m)(L-2) + m(1 + d_1)$ is the number of parameters, where we fix d_0, d_1, L, and m. The fundamental result of Hornick et al. [HSW89] justifies the use of neural networks as function approximators by proving that the set of all feedforward networks letting m vary is dense in $L^2(\nu)$ for any finite measure ν on $\mathbb{R}^d$, whenever ϱ is continuous and non-constant.
In the whole article, we use three hidden layers and a number of neurons equal to $10 + d$ such that the dimensional space for the parameters of the neural network is $\hat{\kappa} = \kappa_{4,10+d}$. Gradient descent is implemented in Tensorflow [Aba+15] using ADAM optimized [KB14]. The activation function used is the tanh function.

3 Mean-Variance efficient frontier in a continuous setting

In this section we suppose that the assets follow a Black Scholes model:

$$\frac{dS_t}{S_t} = \mu dt + \sigma dW_t \tag{3}$$

with S_t with values $\mathbb{R}^d$ with components $S_{t,j}$, $\quad j = 1, \ldots, d$, μ with values in $\mathbb{R}^d$, $\sigma \in \{\text{diag}(v), v \in \mathbb{R}^d_{>0}\}$ the set of diagonal matrices with strictly positive values, $w_t = (\hat{w}^i_t)_{i=1,d}$ where the $\hat{w}^i$ are $\mathcal{F}_t$ adapted Brownian motions correlated with a correlation matrix ρ.
In the continuous setting, we note $\xi = (\xi_t)_{t>0}$ the investment strategy with values in $\mathbb{R}^d$ until maturity T, with a component i corresponding to the fraction of wealth invested in asset i. We suppose ξ_t is in $\mathcal{L}^2_{\mathcal{F}_t}(0, T, \mathbb{R}^d)$. The portfolio value at date T verifies:

$$X^\xi_T = X_0 + \int_0^T \xi_t X^\xi_t . \frac{dS_t}{S_t} = X_0 + \int_0^T X^\xi_t \xi_t . (\mu dt + \sigma dW_t) \tag{4}$$

The Mean-Variance problem consist in finding strategies ξ adapted to the available information that minimize:

$$(J_1(\xi), J_2(\xi)) = (-\mathbb{E}[X^\xi_T], \mathbb{E}[(X^\xi_T - \mathbb{E}[X^\xi_T])^2]). \tag{5}$$

An admissible strategy ξ^* is said to be efficient if there is no other strategy ψ such that

$$J_1(\psi) \leq J_1(\xi^*), \quad J_2(\psi) \leq J_2(\xi^*)$$

and at least one of the two previous inequalities is strict.
Then $(J_1(\xi^*), J_2(\xi^*))$ is an efficient point and the set of all efficient points defines the efficient frontier. By convexity (see [ZL00]), this Pareto frontier can be calculated by minimizing the function defined as the weighted average of the two criteria:

$$J_1(\xi) + \beta J_2(\xi) \tag{6}$$

where the parameter $\beta > 0$ defines a point of the efficient frontier.
In the continuous setting, the solution of the Mean-Variance problem is known explicitly [ZL00],[IP19] and the optimal investment strategy $\alpha_t = \xi_t^* X_t^{\xi^*}$ where ξ^* minimizes (6) and $X_t^{\xi^*}$ is the optimal portfolio associated is given by:

$$\alpha(X_t^{\xi^*}) = -(\sigma\rho\sigma)^{-1}\mu\Big[X_t^{\xi^*} - X_0 - \frac{e^{RT}}{2\beta}\Big], \quad 0 \leq t \leq T \tag{7}$$

where $R = \mu.((\sigma\rho\sigma)^{-1}\mu)$.
The problem (6) does not admit any dynamic programming principal due the average term in the variance definition so that no PDE or regression method can be used directly to solve it. The derivation of the analytic solution is based on a LQ auxiliary equivalent formulation as shown in [ZL00]. Indeed the solution of the problem (6) is solution of

$$\xi^* = \underset{\xi \in \mathcal{L}^2_{\mathcal{F}_t}(0,T,\mathbb{R}^d)}{\operatorname{argmin}} \mathbb{E}[(X_T^{\xi} - \gamma)^2] \tag{8}$$

where

$$\gamma = \frac{1}{2\beta} + \mathbb{E}[X_T^{\xi^*}]. \tag{9}$$

It is then possible to estimate the efficient frontier by the resolution of the problem (8) by letting γ vary. This kind of formulation is generally used by conventional methods such as regressions [CO16] and PDEs [WF10], [DF14] as the dynamic programming principle can be used.

3.1 Neural network approximations

Equation (4) is first discretized on grid of dates $t_i, 0 \leq i < N$ such that $t_0 = 0$, $0 < t_i < T$ for $0 < i < N$ and we note $t_N = T$. We note ϕ^i a position (as a fraction of the wealth invested in each asset) at date t_i, and $\phi = (\phi^i)_{i=0,\dots,N-1}$. The portfolio value is than given by

$$X_T^{\phi} = X_0 + \sum_{i=0}^{N-1} \phi^i X_{t_i}^{\phi} . \frac{S_{t_{i+1}} - S_{t_i}}{S_{t_i}} \tag{10}$$

We first present the methodology used to solve (6) for a given β (or (8) for a given γ). The state of the system only depends on t and the wealth x, then we classically introduce a single network with parameters $\theta \in \mathbb{R}^{\hat{\kappa}}$ taking t and the wealth x as input (so in dimension 2) and with output $\hat{\phi}^{\theta}(t,x)$ in dimension d where $\hat{\phi}_j^{\theta}(t_i,.)$ is an approximation of ϕ_j^i. No activation function is used on the final output such that the network gives an output potentially covering $\mathbb{R}^d$. Then we solve

$$\theta^* = \underset{\theta \in \mathbb{R}^{\hat{\kappa}}}{\operatorname{argmin}} \; -\mathbb{E}[X_T^{\hat{\phi}^{\theta}}] + \beta \mathbb{E}[(X_T^{\hat{\phi}^{\theta}} - \mathbb{E}[X_T^{\hat{\phi}^{\theta}}])^2] \tag{11}$$

for problem (6) or

$$\theta^* = \underset{\theta \in \mathbb{R}^{\hat{\kappa}}}{\operatorname{argmin}} \mathbb{E}[(X_T^{\hat{\phi}^\theta} - \gamma)^2] \tag{12}$$

for problem (8).
Instead of evaluating the frontier by solving (11) for each β chosen (or (12) for each γ), a second resolution method aims at evaluating the global frontier in one calculation. In this case, taking for example problem (6), we introduce a network with input (t, x, β) in dimension 3 and still with an output in dimension d. The associated strategy is noted $\hat{\phi}^{\theta;\beta}$ to emphasize the dependence on β and we solve :

$$\theta^* = \underset{\theta \in \hat{\kappa}}{\operatorname{argmin}} \mathbb{E}[-\mathbb{E}[X_T^{\hat{\phi}^{\theta;\hat{\beta}}}/\hat{\beta}] + \hat{\beta}\mathbb{E}[(X_T^{\hat{\phi}^{\theta;\hat{\beta}}} - \mathbb{E}[X_T^{\hat{\phi}^{\theta;\hat{\beta}}}/\hat{\beta}])^2/\hat{\beta}]] \tag{13}$$

where $\hat{\beta}$ is a random variable with density that can be taken

- either with discrete values so $p(x) = \frac{1}{K}\sum_j^K \delta_{\beta_j}(x)$ where $(\beta_i)_{i=1,K}$ is a set of values where we want to approximate the frontier (generally $\beta_1 = 0$) and in this case it is equivalent to minimize

$$\theta^* = \underset{\theta}{\operatorname{argmin}} \sum_{k=1}^{K} -\mathbb{E}[X_T^{\hat{\phi}^{\theta;\beta_k}}] + \beta_k \mathbb{E}[(X_T^{\hat{\phi}^{\theta;\beta_k}} - \mathbb{E}[X_T^{\hat{\phi}^{\theta;\beta_k}}])^2] \tag{14}$$

- or $p(x)$ is for example an uniform law on $[\underline{\beta}, \bar{\beta}]$ representing where we want to approximate the frontier.

All results in the following section are obtained using some batch of size 300, the linear rate is taken linearly decreasing from $1e-2/d$ to $1e-2/(10d)$ with gradient iterations. The number of iterations is set to 15000. After training using 40 points ($K = 40$ in the global estimation in equation (14), or 40 points to approximate the frontier point by point), each point of the frontier is plotted calculating mean and variance using $1e5$ simulations.

3.2 Results in dimension 4

We take $\mu = (0.01, 0.0225, 0.035, 0.0475)^T$, the diagonal of σ is given by

$$(0.05, 0.1, 0.15, 0.2)$$

and we take

$$\rho = \begin{pmatrix} 1. & 0.26 & -0.43 & 0.233 \\ 0.26 & 1. & 0.003 & 0.06 \\ -0.43 & 0.003 & 1. & -0.33 \\ 0.233 & 0.06 & -0.33 & 1. \end{pmatrix}.$$

We suppose that $T = 1$ year and that the rebalancing is achieved twice a week ($N = 104$) to approach a continuous rebalancing. We plot the frontier obtained with β values between 0.05 to 2.7. The analytic solution is obtained by applying the continuous optimal control (7) at each rebalancing date. In the sequel, in the figures, "Point by point" stands for an approximation using (11), "point by point auxiliary" for an approximation using (12), "global" stands for an approximation using (14), "global random" stands for an approximation using (13) and an uniform law for $\hat{\beta}$. At last "global auxiliary" and "global auxiliary random" stand respectively for a global resolution with deterministic and random γ values for the auxiliary problem (8).

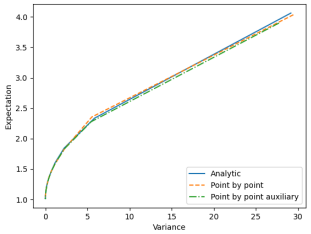

Point by point

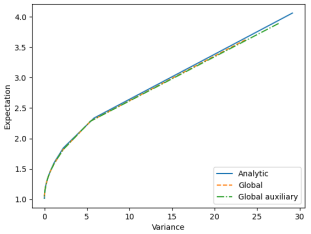

Global

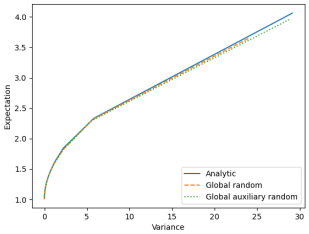

Global random

Figure 1: Efficient frontier in dimension 4.

Results on figure 1 show that the whole frontiers obtained are on the analytic frontier but global estimation on the direct problem (6) tend to fail to reproduce the whole curve. Portfolio with very high returns are not found. Nevertheless results are very good.

3.3 Results in dimension 20

We take $\mu_i = 0.01 + \frac{i-1}{400}$ and the diagonal matrix σ such as $\sigma_{i,i} = 0.05 + \frac{i-1}{100}$ for $i = 1, \ldots, 20$. The correlation is picked up randomly. Results on figure 2 show that the point by point approximation especially for the direct approach is less effective for very small β. The global approach can slightly outperform the analytic solution as the continuous formula is applied on a time discrete problem.

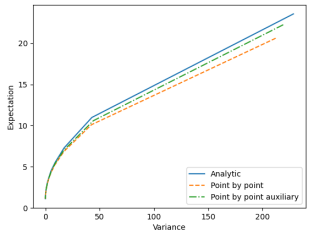

Point by point

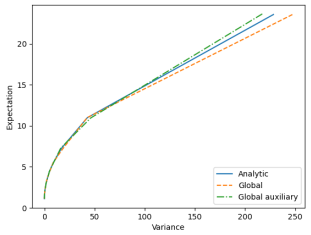

Global

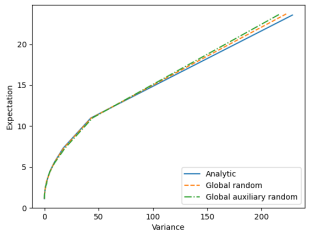

Global random

Figure 2: Efficient frontier in dimension 20.

4 Mean-Variance on the discrete case adding constraints

In the section, on focus on the discrete case still trying to solve (6) or (8).

Remarque 4.1 *We always suppose that the allocation weights belong to a convex set and then* (8) *and* (6) *remain equivalent.*

In the whole section, we impose that there is no short selling, no borrowing and that all the whole wealth is invested. Then in the two sections below, the ϕ^i in equation (10) satisfy:

$$\begin{aligned} &0 \leq \phi_j^i \leq 1, \quad \forall i = 0, \ldots, N-1, \quad j = 1, \ldots, d \\ &\sum_{j=1}^{d} \phi_j^i = 1, \quad \forall i = 0, \ldots, N-1 \end{aligned} \tag{15}$$

In this case, we can rewrite equation (10) by introducing the yield vector $\mathbb{Y}_i = \frac{S_{t_{i+1}} - S_{t_i}}{S_{t_i}}$ so that:

$$X_T^{\phi} = X_0 \prod_{i=0}^{N-1} (1 + \phi_i . \mathbb{Y}_i) \tag{16}$$

In all the cases in this section we take $T = 10$ years and we suppose that rebalancing is achieved once a month. In dimension 4 and 20, trends and volatilities are the same as in the continuous case but correlations are increased and for example in dimension 4:

$$\rho = \begin{pmatrix} 1. & 0.805 & -0.894 & 0.59 \\ 0.805 & 1. & -0.571 & 0.473 \\ -0.894 & -0.571 & 1. & -0.772 \\ 0.59 & 0.473 & -0.772 & 1. \end{pmatrix}.$$

4.1 No other constraints

In this section, we suppose that only constraints (15) are imposed. We use a similar network as in the previous section with parameter θ except that we use a sigmoid activation function at the output giving a network $\hat{\kappa}^{\theta}(t, X)$ for the point by point evaluation with values in $[0, 1]^d$. Investment weights are then given by

$$\hat{\phi}^{\theta}(t, X) = \frac{\hat{\kappa}^{\theta}(t, X)}{\sum_{i=1}^{d} \hat{\kappa}_i^{\theta}(t, X)} \tag{17}$$

Then equation (11) or (12) can be solved.
Similarly for a global formulation the network for the direct problem (6) take (t, x, β) as input and the weights are defined as

$$\hat{\phi}^{\theta;\beta}(t, X, \beta) = \frac{\hat{\kappa}^{\theta}(t, X, \beta)}{\sum_{i=1}^{d} \hat{\kappa}_i^{\theta}(t, X, \beta)}. \tag{18}$$

Then it is possible to solve (13) or to minimize the objective function corresponding to the auxiliary problem.
In the sequel of the article, we will note by static optimization ("Static" on figures) the optimal constant mix strategy such that the weights are kept constant during the whole period. Then the optimization constrained with the weights being constant can be used too to give an efficient frontier in this class of strategies. When "Static" is not specified, a plot is carried out with a dynamic optimization.

Remarque 4.2 *For a static optimization no neural network is used and the problem is reduced to an optimization in dimension d.*

In this section we take an initial learning rate equal to $0.5e - 2/d$ and linearly decreasing with iterations to $0.5e - 2/(10d)$. The number of gradient iterations is set to 15000, the batch size equal to 100.

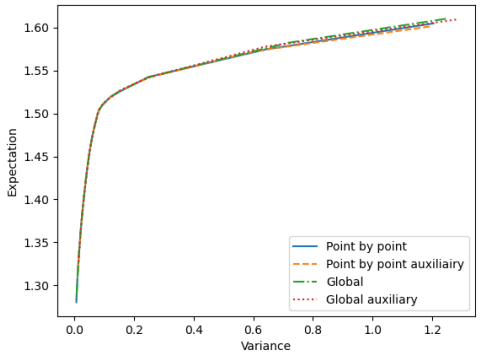

Dimension 4

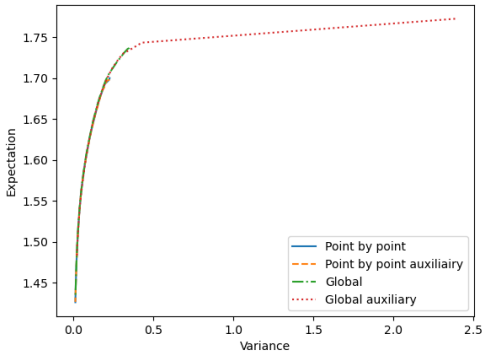

Dimension 20

Figure 3: Efficient frontier with static optimization.

On figure 3, we plot the efficient frontier calculated by static optimization for different methods. In dimension 4, all methods seem to get back the whole frontier while in dimension 20 very high return are hard to catch with most of the methods : only the global auxiliary method can catch the very high returns.

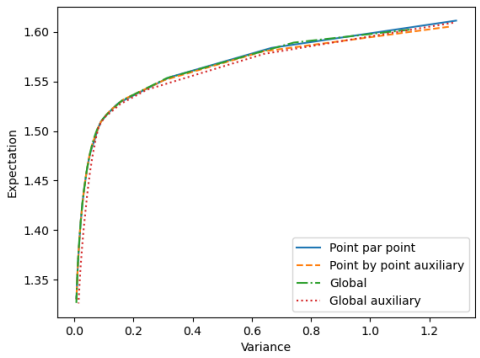

Dimension 4

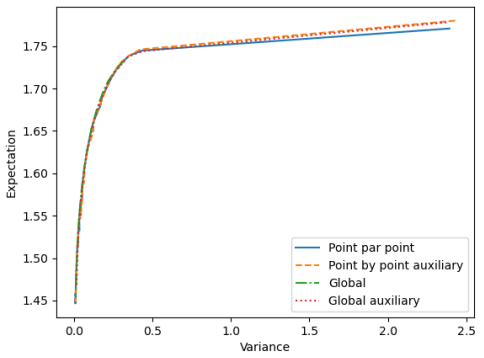

Dimension 20

Figure 4: Efficient frontier with dynamic optimization.

As seen on figure 4 dealing with the dynamic case, global with deterministic β (respectively γ) coefficients and point by point methods give the same results except for very small β values corresponding to very high γ values.
The randomize version of the global approach here doesn't give good results as shown on figure 5: in dimension 4, direct global approach with randomization only give a part of the curve while the auxiliary random version gives another part of the optimal curve. At last in dimension 20, the randomized auxiliary version is sub optimal.

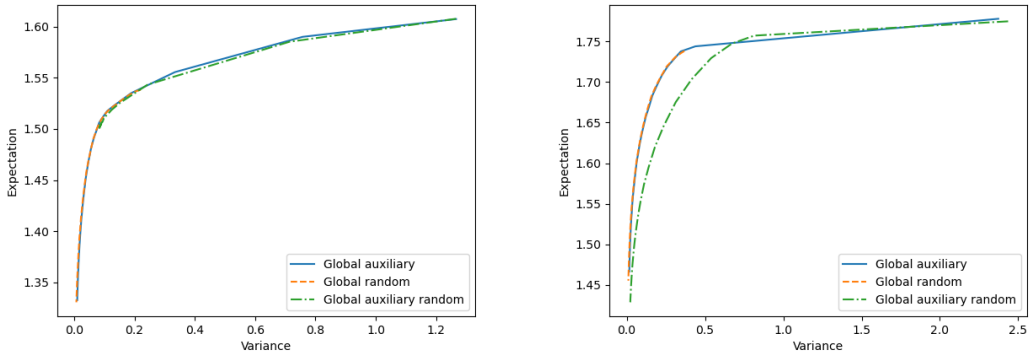

Dimension 4 Dimension 20

Figure 5: Efficient frontier with dynamic optimization for global random approach : methods with stochastic risk coefficients compared to reference calculated with global auxiliary method.

4.2 Adding constraints on the weights

Investors often impose other constraints on portfolio:

- Some are local constraints: the variations of the weights are limited from one step to another in order to face liquidity constraints and to reduce transaction cost:

$$|(\phi_j(t_{i+1}, X_{t_{i+1}}) - \phi_j(t_i, X_{t_i})| \leq \eta_j, \text{ for } j = 1, \ldots, d, \text{ and } i = 0, \ldots, N-1 \tag{19}$$

- Some are global constraints : weights are only allowed to stay in some convex compact:

$$\underline{\phi}_j \leq \phi_j(t_i, X_{t_i}) \leq \bar{\phi}_j, \quad \text{for } j = 1, \ldots, d. \tag{20}$$

We first compare some formulations to solve the problem with the previous constraints. We test them on the point by point estimation of the frontier in dimension 4 in the next subsection. Then we use the best model to achieve an exhaustive comparison of the point by point and global approaches.

4.2.1 Presentation of the different models on the point by point approach in dimension 4

- The first model consists in taking the same representation for the weights as in equation (17). Then constraints (19), (20) are imposed by penalization of the objective function and the parameters θ minimize:

$$J_1(\hat{\phi}^\theta) + \beta J_2(\hat{\phi}^\theta) + \frac{1}{\epsilon} \sum_{j=1}^{d} \sum_{i=0}^{N-2} \mathbb{E}\left[(|\hat{\phi}_j^\theta(t_{i+1}, X_{t_{i+1}}^{\hat{\phi}^\theta}) - \hat{\phi}_j^\theta(t_i, X_{t_i}^{\hat{\phi}^\theta})| - \eta_j)^+ \right] +$$
$$\frac{1}{\epsilon} \sum_{j=1}^{d} \sum_{i=0}^{N-1} \mathbb{E}\left((\hat{\phi}_j^\theta(t_i, X_{t_i}^{\hat{\phi}^\theta}) - \bar{\phi}_j)^+ + (\underline{\phi}_j - \hat{\phi}_j^\theta(t_i, X_{t_i}^{\hat{\phi}^\theta}))^+ \right) \tag{21}$$

where ϵ is a small penalization parameter.

- The second model consists in introducing the variation of weights between two dates similarly as in [FMW19]. We introduce $\xi^\theta(t,X)$ a neural network taking time and the portfolio value as input with an tanh activation function as output so with values in $[-1,1]^d$. The initial portfolio weight is represented by a vector $\tilde{\theta}$ in $\mathbb{R}^d$ and the weight in the portfolio at a given date is given by:

$$\hat{\phi}^{\theta,\tilde{\theta}}(t_i, X_{t_i}^{\hat{\phi}^{\theta,\tilde{\theta}}}) = \tilde{\theta} + \eta \sum_{l=1}^{i} \xi^\theta(t_l, X_{t_l}^{\hat{\phi}^{\theta,\tilde{\theta}}}) \tag{22}$$

We note $\bar{\theta} = (\theta, \tilde{\theta})$. Local constraints are taken into account in this formulation. It remains to impose global bounds on the weights and the constraint on the summation of the weights. It leads to the minimization in $\bar{\theta}$ of

$$J_1(\hat{\phi}^{\bar{\theta}}) + \beta J_2(\hat{\phi}^{\bar{\theta}}) + \frac{1}{\epsilon} \sum_{i=0}^{N-1} \mathbb{E}\left(|\sum_{j=1}^{d} \hat{\phi}_j^{\bar{\theta}}(t_i, X_{t_i}^{\hat{\phi}^{\bar{\theta}}}) - 1| \right)$$
$$\frac{1}{\epsilon} \sum_{j=1}^{d} \sum_{i=0}^{N-1} \mathbb{E}\left((\hat{\phi}_j^{\bar{\theta}}(t_i, X_{t_i}^{\hat{\phi}^{\bar{\theta}}}) - \bar{\phi}_j)^+ + (\underline{\phi}_j - \hat{\phi}_j^{\bar{\theta}}(t_i, X_{t_i}^{\hat{\phi}^{\bar{\theta}}}))^+ \right) \tag{23}$$

- The third model consist in imposing directly the global constraints at the output of the network (22) by introducing:

$$\hat{\phi}^{\theta,\tilde{\theta}}(t_i, X_{t_i}^{\hat{\phi}^{\theta,\tilde{\theta}}}) = (\tilde{\theta} + \eta \sum_{l=1}^{i} \xi^\theta(t_l, X_{t_l}^{\hat{\phi}^{\theta,\tilde{\theta}}})) \wedge \bar{\phi}) \vee \underline{\phi} \tag{24}$$

Local and global constraint on the weights are taken into account and it remains to impose that the sum of the weights is equal to one giving the following expression to minimize in θ:

$$J_1(\hat{\phi}^{\bar{\theta}}) + \beta J_2(\hat{\phi}^{\bar{\theta}}) + \frac{1}{\epsilon} \sum_{i=0}^{N-1} \mathbb{E}\left(|\sum_{j=1}^{d} \hat{\phi}_j^{\bar{\theta}}(t_i, X_{t_i}^{\hat{\phi}^{\bar{\theta}}}) - 1| \right) \tag{25}$$

- The fourth and last model consists in using a feedforward network giving as output $\kappa^\theta(t,X)$ in $[0,1]^d$ by using a sigmoid activation function at the output of the network. A rescaling is achieved to get some weights in $[\underline{\phi}, \bar{\phi}]$ by

$$\hat{\phi}^\theta(t,X) = \underline{\phi} + \kappa^\theta(t,X)(\bar{\phi} - \underline{\phi}). \tag{26}$$

It remains to get an output in the following hyperplane

$$1 = \sum_{i=1}^{d} \hat{\phi}^\theta(t,X), \tag{27}$$

which can be achieved with the following projection algorithm applied on the network:

Algorithm 1 Projection algorithm applied on the output of the network

1: Input : $\hat{\phi}^\theta(t,X)$ with values in $[\underline{\phi}, \bar{\phi}]$
2: **for** $i = 1, d$ **do**
3: $\quad \hat{\phi}_i^\theta(t,X) = [(\hat{\phi}_i^\theta(t,X) + (1 - \sum_{j=1}^{d} \hat{\phi}_j^\theta(t,X))) \wedge \bar{\phi}_i] \vee \underline{\phi}_i$
4: **end for**
5: Return : $\hat{\phi}^\theta(t,X)$ satisfying (27)

The projections are carried out successively in the different directions. In order to avoid having a preferential direction, it is also possible to randomize the loop of the previous algorithm by performing a random permutation of the different visited dimensions.
The objective function to minimize in θ is

$$J_1(\hat{\phi}^\theta) + \beta J_2(\hat{\phi}^\theta) + \frac{1}{\epsilon}\sum_{j=1}^{d}\sum_{i=0}^{N-1}\mathbb{E}\left[(|\hat{\phi}_j^\theta(t_{i+1}, X_{t_{i+1}}^{\hat{\phi}^\theta}) - \hat{\phi}_j^\theta(t_i, X_{t_i}^{\hat{\phi}^\theta})| - \eta_j)^+\right] \tag{28}$$

Remarque 4.3 *In the previous formulations, we have supposed that the initial weights in the portfolio had to be optimized. It is often a data in the problem and then only weights after the initial date have to be optimized.*

We tests the four previous model on the four dimensional test case described at the beginning of the section. We impose the additional constraints : the weights cannot vary more than 0.05 in absolute value between two rebalancing date and we impose that weights are between 0.1 and 0.6. Besides in this case, we impose that initial weights are the same for each asset.
We take the following resolution parameters: we take $\epsilon = 1e-4$, the initial learning rate is set to $1e-3$ and the learning rate decreases to $1e-5$ with the gradient iterations. The batch size is equal to 100. For each case, we carry out 4 optimizations and keep the best result. In the table 1, we give $\mathbb{E}(X_T) - \beta\mathbb{E}((X_T - \mathbb{E}(X_T))^2)$ for the four models for different values of β.

β	0	0.23	0.479	0.719	0.959	1.198	1.427	1.678	2.158
Opt 1	1.468	1.419	1.402	1.392	1.382	1.370	1.365	1.354	1.337
Opt 2	1.336	1.309	1.322	1.334	1.322	1.313	1.298	1.303	1.292
Opt 3	1.397	1.290	1.224	1.206	1.213	1.306	1.167	1.245	0.791
Opt 4	1.474	1.426	1.409	1.398	1.387	1.378	1.368	1.360	1.344

Table 1: Comparison of the 4 models taking into account the constraints giving $E(X_T) - \beta E((X_T - E(X_T))^2)$ obtained.

Models 1 and 4 give the best results. Besides, models 2 and 3 have difficulties to satisfy the constraints: in the following table 1 we give the opposite of the objective function calculated. The difference between results in table below with results in table 1 indicate a violation of the constraints.

β	0	0.23	0.479	0.719	0.959	1.198	1.427	1.678	2.158
Opt 1	1.427	1.371	1.396	1.380	1.373	1.370	1.362	1.354	1.337
Opt 2	1.335	1.307	1.320	1.331	1.318	1.313	1.280	1.281	1.246
Opt 3	-620	-660	-942	-568	-479	-1336	-670	-611	-750
Opt 4	1.474	1.425	1.409	1.397	1.386	1.378	1.368	1.360	1.341

Table 2: Opposite of the objective function.

Model 3 is totally unable to take into account the constraints, while model 2 satisfies globally the constraints. Once again models 1 and 4 are the best to respect the constraints.

4.2.2 Point by point approximation for efficient frontier

We keep model 1 and model 4 to test them further in different dimensions. We suppose that the weights are between $0.5p_{Init}$ and $2p_{Init}$ where $p_{Init} = \frac{1}{d}$ is the initial equal weight used in the portfolio. Local constraints are kept as in the previous subsection with variations below 0.05 in absolute value between two rebalancing date. Optimization parameters are:

- Model 1: initial learning rate equal to $\frac{0.8e-3}{d}$ and linearly decreasing to $\frac{0.8e-3}{10d}$ with gradient iterations,
- Model 4: initial learning rate equal to $1e-3$ and linearly decreasing to $1e-5$.

25000 iterations of gradient are used. The batch size is equal to 100. In dimension 4, the efficient frontier is estimated using 40 discretization points. In dimension 20, 40 discretization points are used with model 1 while 16 points are used only with model 4: it is important to notice that the projection algorithm leads to a computational time far more important as the dimension of the problem increases.

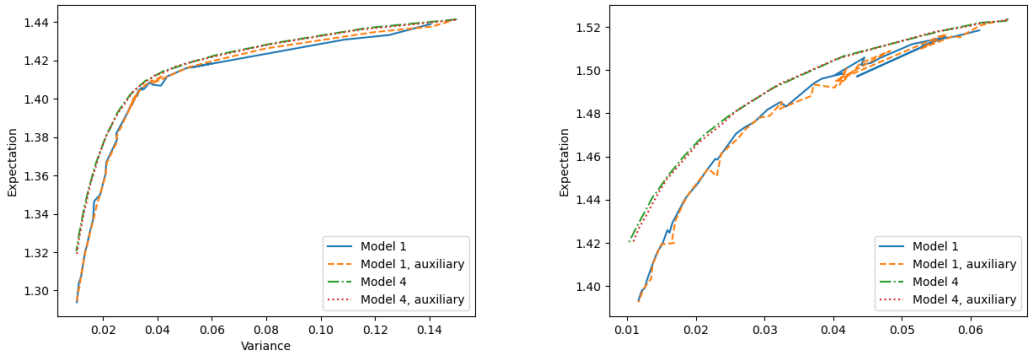

Dimension 4 Dimension 20

Figure 6: Comparing model 1 and 4 to take into account constraints in a point by point approximation of the efficient frontier.

In table 6, we compare model 1 and 4 to calculate the efficient frontier using the direct or auxiliary problem. Direct and auxiliary problems give the same frontier for both methods and model 4 is clearly superior to model 1. In the following model 4 will be used to deal with the global/local constraints.

4.2.3 Global optimization and comparison with point by point optimization of the efficient frontier.

We keep the constraints defined in section 4.2.2. The model 4 can be extended easily to estimate the frontier globally: the network κ^θ with parameters θ is now a function of t, X, β still with values in $[0,1]^d$. The weight approximation is carried out by:

$$\hat{\phi}^{\theta;\beta}(t,X,\beta) = \underline{\phi} + \kappa^\theta(t,X,\beta)(\bar{\phi} - \underline{\phi}). \tag{29}$$

The projection algorithm (27) is used and the objective function (13) is replaced by:

$$\begin{aligned}\theta^* = &\underset{\theta}{\operatorname{argmin}}\, \mathbb{E}[-\mathbb{E}[X_T^{\hat{\phi}^{\theta;\hat{\beta}}}/\hat{\beta}] + \hat{\beta}\mathbb{E}[(X_T^{\hat{\phi}^{\theta;\hat{\beta}}} + \mathbb{E}[X_T^{\hat{\phi}^{\theta;\hat{\beta}}}/\hat{\beta}])^2/\hat{\beta}]] + \\ &\frac{1}{\epsilon}\sum_{j=1}^{d}\sum_{i=0}^{N-2}\mathbb{E}[|\hat{\phi}_j^\theta(t_{i+1}, X_{t_{i+1}}^{\hat{\phi}^\theta;\hat{\beta}}, \hat{\beta}) - \hat{\phi}_j^\theta(t_i, X_{t_i}^{\hat{\phi}^\theta;\hat{\beta}}, \hat{\beta})| - \eta_j)^+]\end{aligned} \tag{30}$$

Off course a similar objective function can be written for the auxiliary problem.
We only present the results obtained using the deterministic (for β and γ) global method as the

randomized approach tends to represent only a part of the curve or is sub optimal as seen on the case without constraints. As before, in dimension 4, 40 points are used to estimate the efficient frontier while only 16 are used in dimension 20.

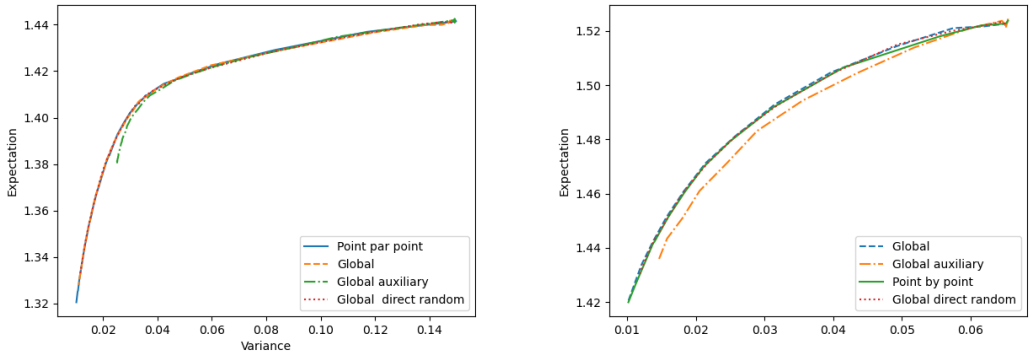

Dimension 4 Dimension 20

Figure 7: Point by point versus global efficient frontier estimation.

On figure 7, we plot the efficient frontier obtained by point by point and global estimation. The point by point calculation and the direct global calculations (deterministic and randomized version) give the same curves in dimension 4 and 20. The global auxiliary approach gives a sub optimal curve in dimension 4 and 20 for its deterministic version while the randomize version gives solution with a flat variance in both cases so is not reported.

Remarque 4.4 *In the whole section, we have added local constraints in the strategies. It is also possible to remove the local constraints and take into account the transaction costs directly in the dynamic of the asset. Supposing that half of spread bid ask for asset i is given by p_i, and still supposing that we deal with the time discrete optimization* (10)*, then the final value of the assets is given with the convention $\phi_{-1} = 0$ by*

$$X_T^\phi = X_0 + \sum_{i=0}^{N-1} \phi_i X_{t_i}^\phi . \frac{S_{t_{i+1}} - S_{t_i}}{S_{t_i}} + \sum_{i=0}^{N-1} \sum_{j=1}^{d} |\frac{\phi_{i,j} X_{t_i}^\phi}{S_{t_i,j}} - \frac{\phi_{i-1,j} X_{t_{i-1}}^\phi}{S_{t_{i-1},j}}| p_j \tag{31}$$

Now the control depends not only on the wealth but also on S_t and the weight at the previous date and they have to be included in the state at the input of the network.

5 Time discrete optimization under an Heston model

We now suppose that the assets follow and Heston model [Hes93]:

$$\begin{aligned} dS_t =& \mu S_t + \sqrt{V_t} S_t dW_t^1, \\ dV_t =& \kappa(\bar{V} - V_t)dt + \bar{\sigma}\sqrt{V_t} dW_t^2 \end{aligned} \tag{32}$$

where S_t, V_t with values in $\mathbb{R}^d$, (W_t^1, W_t^2) is a vector of $2d$ Brownian correlated with a correlation matrix ρ. As there is no analytic solution to equation (32), we rely on a Milstein scheme on the volatility [KJ06] to assure positivity of the volatility under the Feller condition $2\kappa\bar{V} \leq \bar{\sigma}^2$.
We are only interested in the discrete problem with no short selling and no borrowing : weights are all in $[0, 1]$ and the summation of the weights is equal to one. This problem is interesting

as the state of the problem now involve not only the wealth X_t but also the variance V_t, such that not only the control but also the global state has a dimension increasing with the number of assets in the portfolio.
We first deal with the case without additional constraints and then the case with local and global constraints. For all optimizations, we take a learning rate initially equal to $1e-3$ and linearly decreasing to $1e-4$ with stochastic gradient iterations. We take 25000 gradient iterations. The batch size is equal to 100.

5.1 No additional constraints

Using the previous algorithm equation (17) and (18) are now replaced by

$$\hat{\phi}^{\theta}(t, X, V_1, \ldots, V_d) = \frac{\hat{\kappa}^{\theta}(t, X, V_1, \ldots, V_d))}{\sum_{i=1}^{d} \hat{\kappa}_i^{\theta}(t, X, V_1, \ldots, V_d))} \tag{33}$$

for the point by point approximation and by

$$\hat{\phi}^{\theta;\beta}(t, X, V_1, \ldots, V_d, \beta) = \frac{\hat{\kappa}^{\theta}(t, X, V_1, \ldots, V_d, \beta))}{\sum_{i=1}^{d} \hat{\kappa}_i^{\theta}(t, X, V_1, \ldots, V_d, \beta))} \tag{34}$$

in the global method where V_j is the variance of the asset j.
In the whole section we still take $T = 10$ years and a rebalancing every month. In dimension 4 we take the following parameters:

$$\mu = (0.01, 0.0225, 0.035, 0.0475)^T,$$

$\bar{V}$ is taken equal to V_0 and given by $(0.0025, 0.01, 0.0225, 0.04)^T$. Volatility of the variance $\bar{\sigma}$ is given by the diagonal matrix with coefficients $(0.05, 0.1, 0.15, 0.2)$. All the κ values are equal to 0.5. The initial asset values are all equal to one. The correlation matrix associated to $(W_{t,1}^1, \ldots, W_{t,d}^1, W_{t,1}^2, \ldots, W_{t,2}^2)$ is given by

$$\rho = \begin{pmatrix} 1. & -0.383 & 0.3787 & -0.324 & -0.751 & -0.110 & 0.2728 & 0.465 \\ -0.383 & 1. & -0.938 & -0.411 & -0.053 & 0.2763 & -0.2268 & -0.349 \\ 0.378 & -0.9388 & 1. & 0.1455 & -0.051 & -0.398 & 0.249 & 0.401 \\ -0.324 & -0.411 & 0.145 & 1. & 0.655 & 0.329 & -0.264 & -0.048 \\ -0.751 & -0.053 & -0.051 & 0.655 & 1. & -0.172 & -0.464 & -0.105 \\ -0.110 & 0.276 & -0.398 & 0.329 & -0.172 & 1. & 0.044 & -0.348 \\ 0.272 & -0.226 & 0.249 & -0.264 & -0.464 & 0.044 & 1. & -0.580 \\ 0.465 & -0.349 & 0.401 & -0.048 & -0.105 & -0.348 & -0.580 & 1. \end{pmatrix}.$$

In dimension 10 a similar test case is created with quite high correlations. All curves are plotted using 30,points.

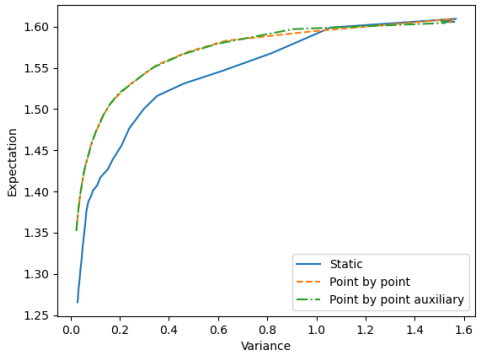

Point by point

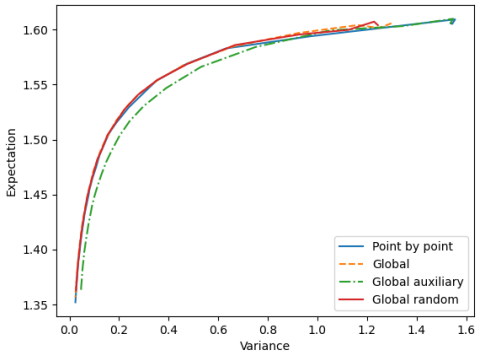

Point by point versus global

Figure 8: Results in dimension 4 for the Heston model without additional constraints.

In figure 8, we first plot in dimension 4 the efficient frontier obtained by direct optimization and using auxiliary equations. Both approaches give the same curve, well above the static curve which surprisingly doesn't seem to be very well estimated (by a point by point approach) as convexity of the curve is not totally respected. In figure 8, we also compare global estimations to point by point estimations: using the direct approach (deterministic and randomized version) we get the same curve as the one given by the point by point estimation. Using the auxiliary version with the global approach, we get similar results as in the Black Scholes case: the deterministic version gives a sub optimal curve while the randomized version is not reported as it gives bad results.
In figure 9, we give the same results in dimension 10. We get very similar results, except that the static point by point optimization curve is more realistic.

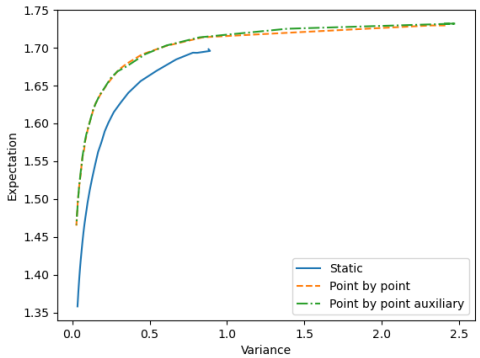

Point by point

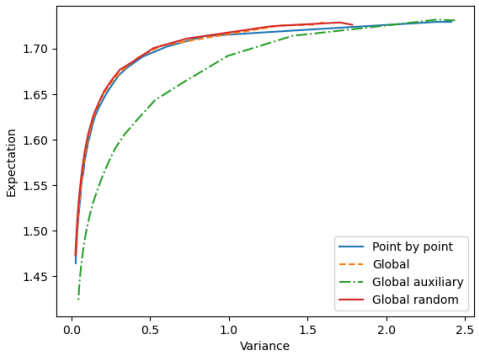

Point by point versus global

Figure 9: Results in dimension 10 for the Heston model without additional constraints.

5.2 Imposing additional local and global constraints

We keep the constraints used in the Black Scholes model in section 4.2.2. The equation (26) is modified taking into account the fact that the state includes the variance of the different assets

for the point by point optimization and the equation (29) is modified in the same way for global optimization.

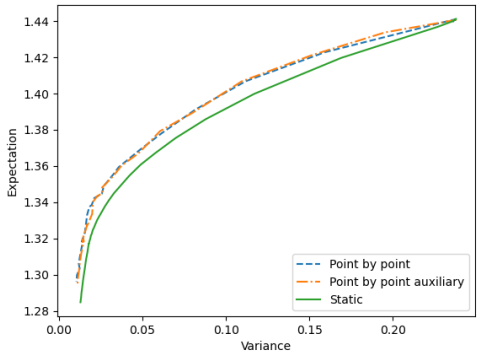

Point by point

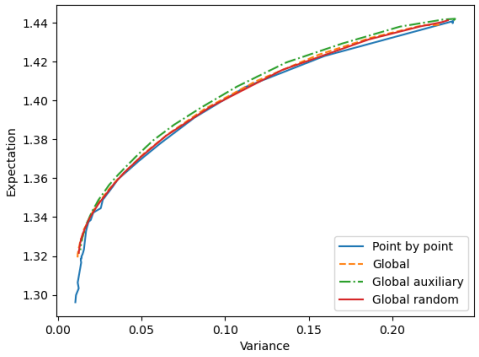

Point by point versus global

Figure 10: Results in dimension 4 for the Heston model with additional constraints.

Figure 10 seems to indicate that we are able to recover the frontier with a good accuracy both by the point by point and the global method.

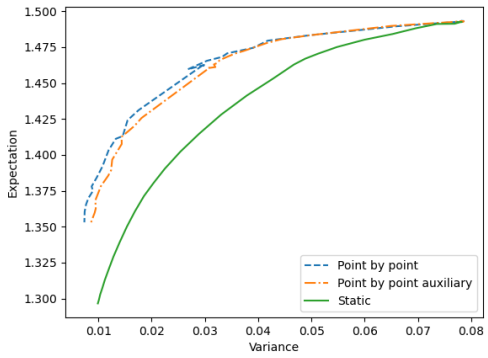

Point by point

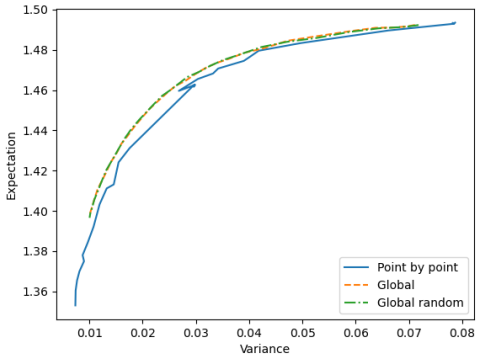

Point by point versus global

Figure 11: Results in dimension 8 for the Heston model with additional constraints.

In higher dimension (for example in figure 11 in dimension 8), the convergence is harder to achieve and small oscillation appear for the point by point approach. In this case, the global auxiliary results are not reported as the curve obtained is not satisfactory. Globally, the global version on the direct approach appears to be the most effective.

6 Mean-CVaR risk optimization

In the whole section we suppose that the assets follow a Black Scholes model given by equation (3). As the Mean-Variance case penalizes both gains and losses, practitioners prefer to use some downsize risk only penalizing the losses (or small gains). In this part we focus on the Mean-CVaR

criterion.
We first recall the VaR definition: if X is a distribution of gain with a continuous cumulative distribution $F_X(x)$ and $\alpha \in]0,1[$, we note

$$VaR(X,\alpha) = \min(y \in \mathbb{R} / P(-X \leq y) \geq \alpha) \tag{35}$$

where $P(-X \leq x)$ is the probability that the random variable $-X$ is below x, so that $P(-X \leq x) = F_{-X}(x)$.
CVaR is then the average loss conditionally to the fact that the losses are above the VaR:

$$CVaR(X,\alpha) = \mathbb{E}[-X/ - X \geq VaR(X,\alpha)] \tag{36}$$

The VaR criterion is not convex but the CVaR is convex [RU+00]. The Mean-CVaR problem consists in finding strategies adapted to the available information and minimizing

$$(J_1(\phi), J_2(\phi)) = (-\mathbb{E}[X_T^\phi], CVaR(X_T^\phi - X_0, \alpha)). \tag{37}$$

where X_T^ϕ is the value of portfolio managed with strategy ϕ and given by (10).
As for the Mean-Variance case, an admissible strategy ϕ^* is efficient if there is no other admissible strategy ψ such that

$$J_1(\psi) \leq J_1(\phi^*), \quad J_2(\psi) \leq J_2(\phi^*)$$

with at least one of the last inequality being strict. The set of efficient points $(J_1(\phi^*), J_2(\phi^*))$ defines the efficient frontier.
As recalled in the introduction, the continuous optimization problem is not well posed and we will only focus on the time discrete optimization problem.
It is also possible to recast the problem as minimizing the CVaR under a constraint that the expected value of the gains is above a threshold M:

$$\min_{\phi \in \mathcal{L}^2_{\mathcal{F}_t}(0,T,\mathbb{R}^d)} CVar(X_T^\phi - X_0)] \tag{38}$$

$$\text{with } E[X_T^\phi] \geq M \tag{39}$$

so that using [RU+00] representation,

$$\min_{y,\phi \in \mathcal{L}^2_{\mathcal{F}_t}(0,T,\mathbb{R}^d)} \mathbb{E}[y + \frac{1}{1-\alpha}(-X_T^\phi + X_0 - y)^+] \tag{40}$$

$$\text{with } E[X_T] \geq M \tag{41}$$

and when optimality is reached, y corresponds to the VaR of the portfolio.
Conventional numerical methods generally prefer this formulation as if y is fixed, the problem can be solved by dynamic programming. Then combining a gradient descent method with this optimization where y is fixed, it possible to optimize the portfolio.
The interest of this formulation is not obvious with neural network problem as it adds a fictitious dimension on the problem and it turns out that using this formulation goes not give good results such that we don't report them in the article.
In the sequel use the same formulation as in the Mean-Variance case: the efficient frontier can be calculated by minimizing (6) using the definition (37) for a fixed β and let β vary to describe the frontier.
As in the Mean-Variance case, it is possible to use a neural network to optimize the strategies by minimize equation (11) for a point by point approximation of the frontier or minimizing the single problem (13) to learn the global curve.
In all the tests, the parameters of the model are the same as in section 4. As before, $T = 10$

years and rebalancing is achieved every month.
As for the convergence of the stochastic gradient, the learning rate starts at $1e-5$ and decreases linearly with gradient iterations to $1e-5$. The number of stochastic gradient iterations is fixed at 15000. The batch size is chosen equal to 2000 to have a correct assessment of the CVaR. While calculating the curve point by point or globally with deterministic β, the following values $\beta_i = (i2/K)^2$, $i = 0, \dots, K-1$ are used. The value for K depends on the case. When a randomization of the parameter β is used, $\hat{\beta} \sim \beta_{K-1} U^2$ where U is an uniform random variable on $[0, 1]$.

6.1 Not short selling, no borrowing

Similarly to the Mean-Variance we can impose some constraints on the portfolio: using the weights formulation (17) while optimizing (6), the weights formulation (18) optimizing (13), it is possible to impose that all weights are positive, between 0 and 1 and with sum equal to one. We train the network and plot the resulting efficient frontier using 40 points first in dimension 4 on figure 12. The global approaches with deterministic and stochastic β give the same curve. The point by point curve appears to be oscillating and may not be very accurate.

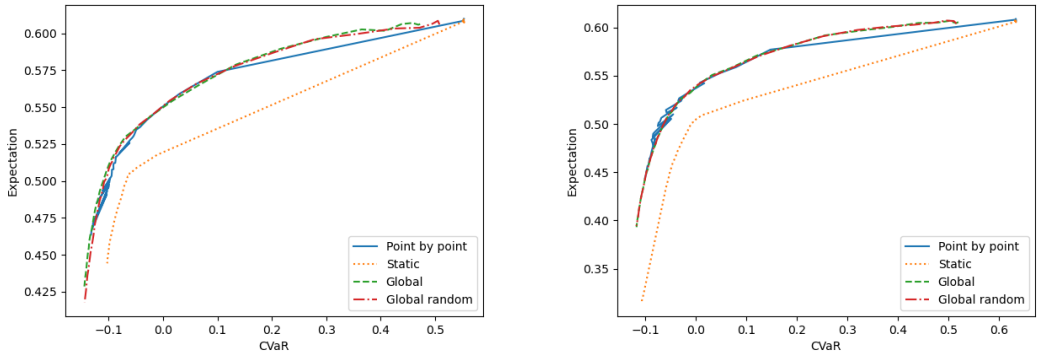

$\alpha = 0.9$ $\alpha = 0.95$

Figure 12: Mean-CVaR optimization comparison between point by point by point optimization with global optimization with deterministic and stochastic β in dimension 4.

In dimension 20, results with point by point approximation are not reported as they give oscillations. Only global solution with deterministic and stochastic β are given on figure 13.

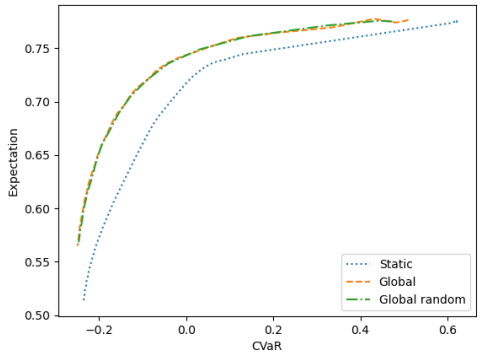

$\alpha = 0.9$

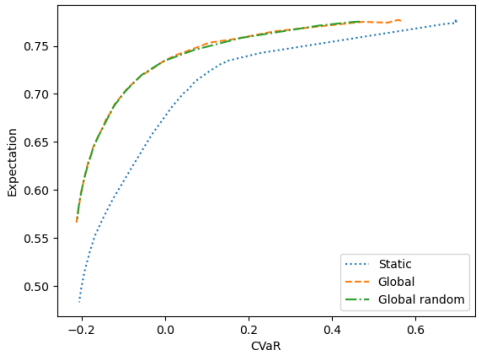

$\alpha = 0.95$

Figure 13: Mean-CVaR optimization comparison between static optimization and global optimization with deterministic and stochastic β in dimension 20.

For the Mean-CVaR criterion, it seems that the global approximation gives the best results.

6.2 Adding other constraints

Using equation (26) with algorithm 1 in equation (28), or equation (29) for the weights while optimizing (30), it is possible to add the constraints given by equations (19) and (20). The parameters for the additional constraints are the same as in section 4.2.2. Results are reported in dimension 4 and only in dimension 8 as computing cost grows significantly with the dimension of the problem. Curves are reconstructed with 20 points. On figure 14, we plot the curves obtained with a static optimization, and the dynamic optimization with the global approaches and the point by point approach. The global approaches seem to give slightly better results.

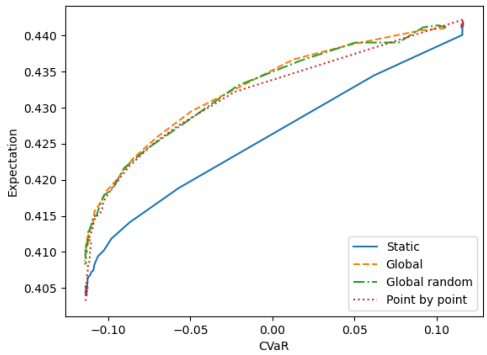

$\alpha = 0.9$

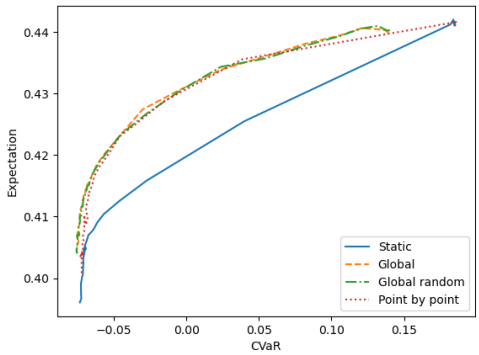

$\alpha = 0.95$

Figure 14: Mean-CVaR in dimension 4 with additional constraints on weights : global, point by point, and static estimations.

In higher dimension, the point by point approach appears to give oscillations. It turns out that the best solution is given by the global approach with random β coefficients as shown on figure 15.

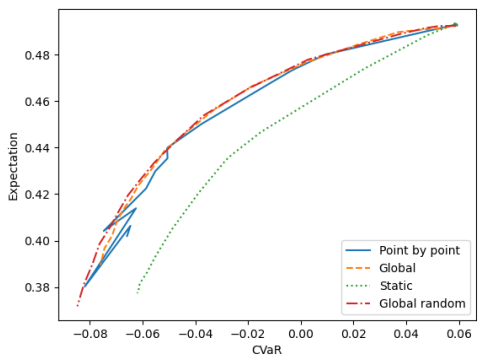

$\alpha = 0.9$

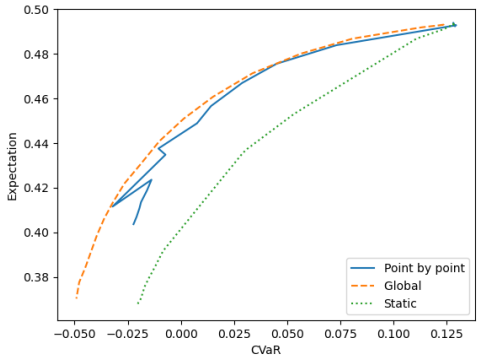

$\alpha = 0.95$

Figure 15: Mean CVaR in dimension 8 with additional constraints on weights : global, point by point, and static estimations.

For example, with $\alpha = 0.95$, some global resolution can lead to some sub optimal curve as shown on figure 16. The optimizer is trapped in a local minimum away from the solution and point by point estimations oscillates between the two curves.

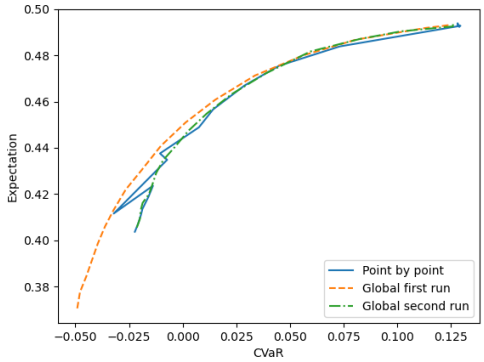

Figure 16: Different Mean CVaR runs with deterministic global method compared to point by point estimation with $\alpha = 0.95$.

So it seems that in all the cases, with or without additional constraints, the global approach is more effective than the point by point approach.

References

[Aba+15] Martin Abadi et al. *TensorFlow: Large-Scale Machine Learning on Heterogeneous Systems*. Software available from tensorflow.org. 2015. URL: `https://www.tensorflow.org/`.

[Bue+19] Hans Buehler et al. "Deep hedging". In: *Quantitative Finance* 19.8 (2019), pp. 1271–1291.

[CO16] Fei Cong and Cornelis W Oosterlee. "Multi-period mean–variance portfolio optimization based on Monte-Carlo simulation". In: *Journal of Economic Dynamics and Control* 64 (2016), pp. 23–38.

[CW14] Mei Choi Chiu and Hoi Ying Wong. "Mean–variance portfolio selection with correlation risk". In: *Journal of Computational and Applied Mathematics* 263 (2014), pp. 432–444.

[DF14] Duy-Minh Dang and Peter A Forsyth. "Continuous time mean-variance optimal portfolio allocation under jump diffusion: An numerical impulse control approach". In: *Numerical Methods for Partial Differential Equations* 30.2 (2014), pp. 664–698.

[DR99] Ron Dembo and Dan Rosen. "The practice of portfolio replication. A practical overview of forward and inverse problems". In: *Annals of Operations Research* 85 (1999), pp. 267–284.

[Fis77] Peter C Fishburn. "Mean-risk analysis with risk associated with below-target returns". In: *The American Economic Review* 67.2 (1977), pp. 116–126.

[FMW19] Simon Fécamp, Joseph Mikael, and Xavier Warin. "Risk management with machine-learning-based algorithms". In: *arXiv preprint arXiv:1902.05287* (2019).

[Gao+17] Jianjun Gao et al. "Dynamic mean-LPM and mean-CVaR portfolio optimization in continuous-time". In: *SIAM Journal on Control and Optimization* 55.3 (2017), pp. 1377–1397.

[GJR18] Jim Gatheral, Thibault Jaisson, and Mathieu Rosenbaum. "Volatility is rough". In: *Quantitative Finance* 18.6 (2018), pp. 933–949.

[Hes93] Steven L Heston. "A closed-form solution for options with stochastic volatility with applications to bond and currency options". In: *The review of financial studies* 6.2 (1993), pp. 327–343.

[HSW89] K. Hornik, M. Stinchcombe, and H. White. "Multilayer feedforward networks are universal approximators". In: *Neural Networks* 2.5 (1989), pp. 359–366.

[IP19] A. Ismail and H. Pham. "Robust Markowitz mean-variance portfolio selection under ambiguous covariance matrix". In: *Mathematical Finance* 29.174-207 (2019).

[JMP20] Eduardo Abi Jaber, Enzo Miller, and Huyên Pham. "Markowitz portfolio selection for multivariate affine and quadratic Volterra models". In: *Available at SSRN 3636794* (2020).

[JYZ05] Hanqing Jin, Jia-An Yan, and Xun Yu Zhou. "Continuous-time mean–risk portfolio selection". In: *Annales de l'Institut Henri Poincare (B) Probability and Statistics*. Vol. 41. 3. Elsevier. 2005, pp. 559–580.

[KB14] Diederik P Kingma and Jimmy Ba. "Adam: A method for stochastic optimization". In: *arXiv preprint arXiv:1412.6980* (2014).

[KJ06] Christian Kahl and Peter Jäckel. "Fast strong approximation Monte Carlo schemes for stochastic volatility models". In: *Quantitative Finance* 6.6 (2006), pp. 513–536.

[KT20] Thomas Krabichler and Josef Teichmann. "Deep Replication of a Runoff Portfolio". In: *arXiv preprint arXiv:2009.05034* (2020).

[Lim04] Andrew EB Lim. "Quadratic hedging and mean-variance portfolio selection with random parameters in an incomplete market". In: *Mathematics of Operations Research* 29.1 (2004), pp. 132–161.

[LN00] Duan Li and Wan-Lung Ng. "Optimal dynamic portfolio selection: Multiperiod mean-variance formulation". In: *Mathematical finance* 10.3 (2000), pp. 387–406.

[LZL02] Xun Li, Xun Yu Zhou, and Andrew EB Lim. "Dynamic mean-variance portfolio selection with no-shorting constraints". In: *SIAM Journal on Control and Optimization* 40.5 (2002), pp. 1540–1555.

[Mar52] H. Markowitz. "Portfolio selection". In: *J Finance* 7.77–91 (1952).

[Mar59] H. Markowitz. *Portfolio Selection: Efficient Diversification of Investment*. Wiley, New York, 1959.

[Mer72] Robert C Merton. "An analytic derivation of the efficient portfolio frontier". In: *Journal of financial and quantitative analysis* (1972), pp. 1851–1872.

[MY17] Christopher W Miller and Insoon Yang. "Optimal control of conditional value-at-risk in continuous time". In: *SIAM Journal on Control and Optimization* 55.2 (2017), pp. 856–884.

[Roy52] Andrew Donald Roy. "Safety first and the holding of assets". In: *Econometrica: Journal of the econometric society* (1952), pp. 431–449.

[RU+00] R Tyrrell Rockafellar, Stanislav Uryasev, et al. "Optimization of conditional value-at-risk". In: *Journal of risk* 2 (2000), pp. 21–42.

[WF10] Jian Wang and Peter A Forsyth. "Numerical solution of the Hamilton–Jacobi–Bellman formulation for continuous time mean variance asset allocation". In: *Journal of Economic Dynamics and control* 34.2 (2010), pp. 207–230.

[ZL00] Xun Yu Zhou and Duan Li. "Continuous-time mean-variance portfolio selection: A stochastic LQ framework". In: *Applied Mathematics and Optimization* 42.1 (2000), pp. 19–33.